Int. J. Appl. Math. Comput. Sci., 2006, Vol. 16, No. 3, 345–356

A ROBUST CONTROLLER DESIGN METHOD AND STABILITY ANALYSIS OF AN UNDERACTUATED UNDERWATER VEHICLE

CHENG SIONG CHIN, MICHEAL WAI SHING LAU
EICHER LOW, GERALD GIM LEE SEET

Robotic Research Centre, Department of Mechanical and Aerospace Engineering
Nanyang Technological University, Singapore 639798
e-mail: mcschin1@yahoo.com

The problem of designing a stabilizing feedback controller for an underactuated system is a challenging one since a nonlinear system is not stabilizable by a smooth static state feedback law. A necessary condition for the asymptotical stabilization of an underactuated vehicle to a single equilibrium is that its gravitational field has nonzero elements corresponding to unactuated dynamics. However, global asymptotical stability (GAS) cannot be guaranteed. In this paper, a robust proportional-integral-derivative (PID) controller on actuated dynamics is proposed and unactuated dynamics are shown to be global exponentially bounded by the Sørdalen lemma. This gives a necessary and sufficient condition to guarantee the global asymptotic stability (GAS) of the URV system. The proposed method is first adopted on a remotely-operated vehicle RRC ROV II designed by the Robotic Research Centre in the Nanyang Technological University (NTU). Through the simulation using the ROV Design and Analysis toolbox (RDA) written at the NTU in the MATLAB/SIMULINK environment, the RRC ROV II is robust against parameter perturbations.

Keywords: underwater vehicle, underactuated, stabilizable, robust controller, simulation

1. Introduction

In this paper, a nonlinear system consisting of actuated and unactuated dynamics is studied. The problem of designing a stabilizing feedback controller for underactuated systems is a challenging one since the system is not stabilizable by a smooth static state feedback law (Brockett, 1983). Fossen (1994) and Yuh (1990) showed that a fully actuated vehicle (a vehicle where the control and configuration vector have the same dimension) can be asymptotically stabilized in position and velocity by a smooth feedback law. Byrnes *et al.* (1991) explained why underactuated vehicles having zero gravitational field are not asymptotically stabilizable to a single equilibrium. On the other hand, Wichlund *et al.* (1995) stated that the vehicle with gravitational and restoring terms in unactuated dynamics is stabilizable to a single equilibrium point. However, it is a necessary but not sufficient condition to state that the vehicle is asymptotically stabilizable. The closed-loop asymptotical stability of the vehicle in the earth-fixed frame needs to be examined further.

A different method than those proposed in (Wichlund *et al.*, 1995) is used to show that actuated dynamics in the earth-fixed frame is exponentially decaying under the nonlinear controller. The method described in (Wichlund *et al.*, 1995) uses a nonlinear dynamic control law to achieve a neat closed loop actuated subsystem that yields an exponentially decaying solution, but gives low flexibility in designing the control law since nonlinear vehicle dynamics have to be known exactly for nonlinear dynamic cancellation.

In this paper, a robust Proportional-Integral-Derivative (PID) controller is chosen due to its simplicity in implementation and its common use in industry. PID is designed only for actuated dynamics, such that it provides a necessary and sufficient condition for the asymptotic stability of unactuated dynamics. In this method, unactuated dynamics are self-stabilizable and converge exponentially to zero. With the controller, the actuated dynamics become asymptotically stable while the actuated states in the unactuated dynamic equation diminish. Applying the asymptotic stability lemma by Sørdalen (Søodalen and Egeland 1993; 1995; Sørdalen *et al.*, 1993) to the unactuated dynamic equation provides a validation for the initial argument of convergence to zero. Thus the vehicle in the earth-fixed frame, which is self-stabilizable in unactuated dynamics, is asymptotically stable.

The paper is organized as follows: A nonlinear model of an underactuated ROV, developed by the Robotic Research Centre in the Nanyang Technological University (Koh *et al.*, 2002b; Micheal *et al.*, 2003), is presented in Section 2. Section 3 describes a necessary con-

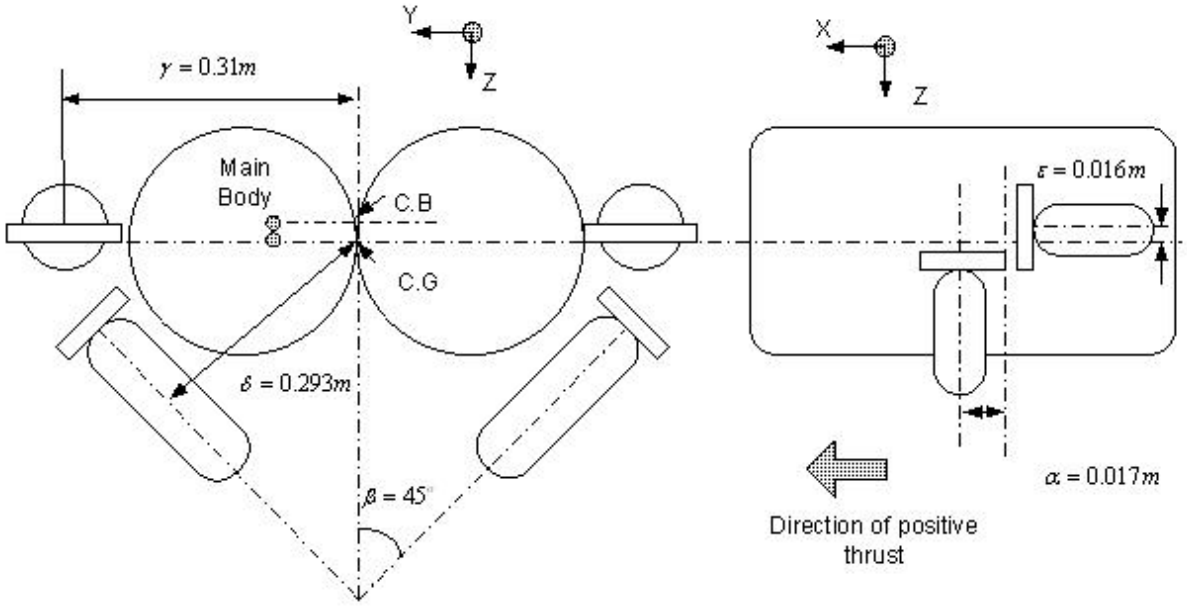

Front view of the RRC ROV II Side view of the RRC ROV II

Fig. 1. Thruster configuration on the ROV platform.

dition for a vehicle with gravitational and restoring terms in unactuated dynamics to be stabilizable. In Sections 4 and 5, a robust PID controller is proposed for the asymptotic stability of the vehicle in the earth-fixed frame which is self-stabilizable in unactuated dynamics. The results of computer simulations using the ROV Design and Analysis (RDA) toolbox written at the NTU in the MATLAB/SIMULINK environment are presented in Section 6.

2. Nonlinear Model of the Underactuated ROV

The dynamic behavior of an underwater vehicle is designed through Newton's laws of linear and angular momentum. The equations of motion of such vehicles are highly nonlinear (Fossen, 1994) and coupled due to hydrodynamic forces which act on the vehicle. Usually, the ROV model can be described in either a body-fixed or an earth-fixed frame.

2.1. Body-Fixed Model of the Underactuated ROV. It is convenient to write the general dynamic and kinematic equations for the ROV in the body-fixed frame:

$$M_v\dot{v} + C_v(v)v + D_v(v)v + g(\eta) = B_v u_v, \quad (1)$$

$$\dot{\eta} = J(\eta)v, \quad (2)$$

where $B_v \in \mathbb{R}^{6\times 4}$ is a thruster configuration matrix (defined by the thruster layout as shown in Fig. 1), $u_v \in \mathbb{R}^4$ is an input vector, $v = [u, v, w, p, q, r]^T \in \mathbb{R}^6$ is a velocity vector, $\eta = [x, y, z, \phi, \theta, \psi]^T \in \mathbb{R}^3 \times S^3$ is a position and orientation vector, $M_v \in \mathbb{R}^{6\times 6}$ is a mass inertia matrix with added mass coefficients, $C_v(v) \in \mathbb{R}^{6\times 6}$ is a centripetal and Coriolis matrix with added mass coefficients, $D_v(v) \in \mathbb{R}^{6\times 6}$ is a diagonal hydrodynamic damping matrix, and $g(\eta) \in \mathbb{R}^6$ is a vector of buoyancy and gravitational forces and moments. The ROV path relative to the earth-fixed reference frame is given by the kinematic equation (2), where $J(\eta) = J(\eta_2) \in \mathbb{R}^{6\times 6}$ and $\eta_2 = [\phi, \theta, \psi]^T$ is an Euler transformation matrix.

2.2. An Earth-Fixed Model of the Underactuated ROV. Sometimes, we need to express the ROV model from the body coordinate to earth-fixed coordinates (Fossen, 1994) by performing the coordinate transformation $(\eta, v) \overset{\mu}{\mapsto} (\eta, \dot{\eta})$ defined by

$$\begin{bmatrix} \eta \\ \dot{\eta} \end{bmatrix} = \begin{bmatrix} I & 0 \\ 0 & J(\eta) \end{bmatrix} \begin{bmatrix} \eta \\ v \end{bmatrix}, \quad (3)$$

where the transformation matrix, J, has the following form:

$$J(\eta) = \begin{bmatrix} c(\psi)c(\theta) & -s(\psi)c(\phi) + c(\psi)s(\theta)s(\phi) \\ s(\psi)c(\theta) & c(\psi)c(\theta) + s(\phi)s(\theta)s(\psi) \\ -s(\theta) & c(\theta)s(\phi) \\ 0 & 0 \\ 0 & 0 \\ 0 & 0 \end{bmatrix}$$

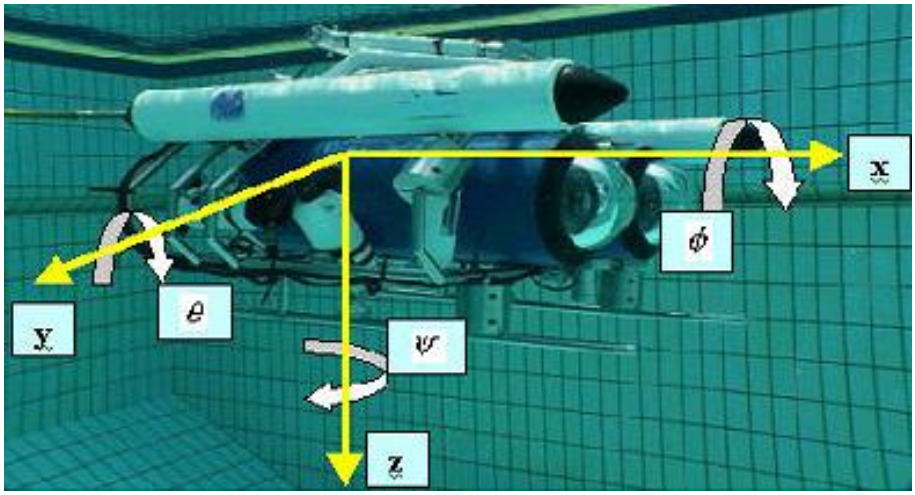

Fig. 2. Experimental RRC ROV II in a swimming pool.

$$\begin{bmatrix} s(\psi)s(\phi)+c(\psi)c(\phi)s(\theta) & 0 & 0 & 0 \\ -c(\psi)s(\phi)+s(\theta)s(\psi)c(\phi) & 0 & 0 & 0 \\ c(\theta)c(\phi) & 0 & 0 & 0 \\ 0 & 1 & s(\phi)t(\theta) & c(\phi)t(\theta) \\ 0 & 0 & c(\phi) & -s(\phi) \\ 0 & 0 & s(\phi)/c(\theta) & c(\phi)/c(\theta) \end{bmatrix}, \quad (4)$$

where $c(\cdot)=\cos(\cdot)$, $t(\cdot)=\tan(\cdot)$ and $s(\cdot)=\sin(\cdot)$. The coordinate transformation μ is a global diffeomorphism which is analogous to a similarity transformation in linear systems. This transformation is undefined for $\theta=\pm 90^o$. To overcome this singularity, a quaternion approach must be considered. However, in our study this problem does not exist because the vehicle is not sufficient to operate at $\theta=\pm 90^o$. Moreover, the vehicle is completely stable in roll and pitch, and the thruster actuation is not sufficient to move the vehicle to operate at this angle. The ROV model in earth-fixed coordinates becomes

$$M_\eta(\dot\eta,\eta)\ddot\eta + C_\eta(\dot\eta,\eta)\dot\eta + D_\eta(\dot\eta,\eta)\dot\eta + g_\eta(\eta) = B_\eta u_\eta, \quad (5)$$

where $M_\eta(\dot\eta,\eta)=J^{-T}M_vJ^{-1}$, $C_\eta(\dot\eta,\eta)=J^{-T}(C-M_vJ^{-1}\dot J)J^{-1}$, $D_\eta(\dot\eta,\eta)=J^{-T}D_v\ J^{-1}$, $g_\eta(\eta)=J^{-T}g_v$ and $B_\eta u_\eta=J^{-T}B_vu_v$.

3. Stabilizability

In this section a method to test system stabilizability is presented. In general, the vector $g_(\eta)$ can be further decomposed into elements corresponding to actuated dynamics (the first to third and sixth elements), $g_a(\eta)$, and the element corresponding to unactuated dynamics (the fourth and fifth elements), $g_u(\eta)$. The proof of Theorem 3 in (Wichlund *et al.*, 1995) regards the system given by Eqns. (1) and (2). Suppose that $(\eta,v)=(0,0)$ is an equilibrium point of the system. If $g_u(\eta)$ is zero, then there exists no continuous and discontinuous state feedback law (Byrnes and Isidori, 1991), $k(\eta,v):\mathbb{R}^6\Rightarrow\mathbb{R}^4$, which makes $(0,0)$ an asymptotically stable equilibrium.

However, the RRC ROV II of Fig. 2 has a gravitational field at unactuated dynamics, $g_u(\eta)=[29.61\cos\theta\sin\phi\ \ 29.61\sin\theta]^T\neq 0$ but no gravitational field at $g_a(\eta)=0$. Therefore, the RRC ROV II may be stabilizable at the equilibrium point. However, it is a necessary, but not sufficient, condition to state that the ROV is asymptotically stabilizable at the equilibrium point. Inevitably, it gives rise to the need of finding a control law to stabilize the ROV at the equilibrium point.

4. Asymptotic Stabilization of Actuated Dynamics by Smooth State Feedback

In Sections 4 and 5, the concepts in the asymptotic stabilization of actuated dynamics are as follows: (i) by observation, the unactuated dynamics in (7) are self-stabilizable and exponentially decaying; (ii) use a robust PID controller to globally asymptotically stabilize the actuated dynamics in (6); (iii) with actuated dynamics, globally asymptotically stable (GAS) f_1 implies that the actuated dynamics h_2 in the unactuated equation (7) becomes zero; (iv) finally, step (i) is verified by the Sørdalen lemma. For clarity, this section is divided into two parts. The problem definition is given in Part I, perturbation on the ROV's parameters and the controller design and the stability analysis on actuated dynamics are provided in Part II.

4.1. Problem Definition. The separation of the entire system into actuated and unactuated subsystems, as de-

scribed in (Micheal *et al.*, 2003), yields

$$\ddot{\eta}_a = f_1(\dot{\eta}_a, \eta_a, t) + h_1(\dot{\eta}_u, \eta_u, t) + B_{\eta_a} u_a, \quad (6)$$

$$\ddot{\eta}_u = f_2(\dot{\eta}_u, \eta_u, t) + h_2(\dot{\eta}_a, \eta_a, t) + B_{\eta_u} u_u, \quad (7)$$

where

$$\begin{aligned} f_1(\dot{\eta}_a, \eta_a, t) &= -\frac{1}{\det(M_\eta)} M_{\eta_{22}} \\ &\quad \times \left[C_{\eta_{11}}(v,\eta) + D_{\eta_{11}}(v,\eta)\right]\dot{\eta}_a, \\ h_1(\dot{\eta}_u, \eta_u, t) &= -\frac{1}{\det(M_\eta)} M_{\eta_{12}} g_{\eta_u} \\ &\quad + M_{\eta_{12}} C_{\eta_{21}}(v,\eta)\dot{\eta}_u, \\ f_2(\dot{\eta}_u, \eta_u, t) &= -\frac{1}{\det(M_\eta)} M_{\eta_{11}} \\ &\quad \times \left[C_{\eta_{22}}(v,\eta) + D_{\eta_{22}}(v,\eta)\right]\dot{\eta}_u, \\ h_2(\dot{\eta}_a, \eta_a, t) &= -\frac{1}{\det(M_\eta)} M_{\eta_{11}} g_{\eta_u} \\ &\quad - M_{\eta_{12}} C_{\eta_{12}}(v,\eta)\dot{\eta}_a, \\ \det(M_\eta) &= M_{\eta_{22}} M_{\eta_{11}} - {M_{\eta_{12}}}^2, \end{aligned}$$

$\eta = [z\ x\ y\ \psi \mid \phi\ \theta]^T = [\eta_a \mid \eta_u]$, $\eta_a \in \mathbb{R}^3 \times S, \eta_u \in \mathbb{R}^2$, $B_\eta = [B_{\eta_a}\ B_{\eta_u}]$ are the input matrices for the actuated and unactuated dynamics in (5). Note that the subscripts 'a' and 'u' refer to the actuated and unactuated dynamics, respectively.

Let η_d denote the desired set points (position and orientation) in the earth-fixed frame. The error of this actuated position about the hovering or station-keeping condition can be written down as

$$e = \eta_a - \eta_d \Rightarrow \dot{e} = \dot{\eta}_a, \quad \ddot{e} = \ddot{\eta}_a. \quad (8)$$

Substituting the preceding equation into (6) and (7) yields

$$\ddot{e} = f_1(\dot{e}, e, t) + h_1(\dot{\eta}_u, \eta_u, t) + B_{\eta_a} u_a, \quad (9)$$

$$\ddot{\eta}_u = f_2(\dot{\eta}_u, \eta_u, t) + h_2(\dot{e}, e, t) + B_{\eta_u} u_u. \quad (10)$$

Consider $h_1(\dot{\eta}_u, \eta_u, t)$ as a perturbation to (9) and assume that it could converge (or exponentially decay) to zero as time increases. Then (9) becomes

$$\ddot{e} = f_1(\dot{e}, e, t) + B_{\eta_a} u_a. \quad (11)$$

The quantity $h_1(\dot{\eta}_u, \eta_u, t)$ decays in (9) as the restoring forces (based on the ROV design intention) in the $\eta_u = \{\phi, \theta\}$ directions enable these two motions to stabilize themselves effectively instead of destabilizing the system. Furthermore, if η_a can be proven to be asymptotically stable, i.e., $e \to 0$ as $t \to 0$, the term $h_2(\dot{e}, e, t)$ in (10) decays and becomes

$$\ddot{\eta}_u = f_2(\dot{\eta}_u, \eta_u, t) + B_{\eta_u} u_u. \quad (12)$$

Applying the asymptotic stability proof for η_u validates the initial assumption of $h_1(\dot{\eta}_u, \eta_u, t) \to 0$ as $t \to \infty$. The following will illustrate the above-mentioned method.

Assuming that the perturbation $h_1(\dot{\eta}_u, \eta_u, t)$ is bounded by a decaying exponential function and $u_a = u_{PID} = -B_{\eta_a}^{-1}(K_p e + K_i \int_0^\tau e\,\mathrm{d}t + K_d \frac{\mathrm{d}e}{\mathrm{d}t})$ for the actuated subsystem exists, (9) becomes $\ddot{e} = f_1(\dot{e}, e, t) + B_{\eta_a} u_{PID}$. The asymptotical stability of η_a, i.e., $e \to 0$ as $t \to 0$ is proven in the following.

4.2. Perturbation on the ROV's Parameters. To test the robustness of PID control schemes, the ROV's mass inertia, centripetal and Coriolis matrix and the diagonal hydrodynamic damping matrix are allowed to vary within the limits specified in (14) and (16). These variations can be attributed to the inaccuracy in modeling and possible changes in the mass distribution in the ROV. The limits were obtained using a computer-aided design (CAD) software, Pro-E. By changing the mass properties of each thruster, pod and stainless-steel frame as shown in Fig. 2, a different mass inertia matrix was obtained. By evaluating the differences between the nominal and new mass inertia matrices, the following limits can be determined:

The bounds $\underline{m_{\eta_1}}$ and $\overline{m_{\eta_1}}$ are obtained by first evaluating the inverse of the body-fixed mass inertia matrix, M_v^{-1} in (5) obtained from the CAD software, Pro-E:

$$M_\eta(\dot{\eta}, \eta) = J^{-T} M_v J^{-1},$$

$$M_\eta(\dot{\eta}, \eta)^{-1} = J M_v^{-1} J^T. \quad (13)$$

Substituting M_v^{-1} that ranges from -0.001 to 0.01 at $J = I$ (as the Euler angles are small) in (4) results in $\underline{m_{\eta_1}} = -0.001$ and $\overline{m_{\eta_1}} = 0.01$. Hence, the bounds on $M_{\eta_1}^{-1}$ become

$$\underline{m_{\eta_1}} I \le M_{\eta_1}^{-1} \le \overline{m_{\eta_1}} I, \quad (14)$$

where

$$M_{\eta_1}^{-1} = M_{\eta_{22}} \left[M_{\eta_{22}} M_{\eta_{11}} - {M_{\eta_{12}}}^2\right]^{-1}. \quad (15)$$

The upper bounds on the centripetal and Coriolis matrix and the diagonal hydrodynamic damping matrix in C_{η_1} are set as

$$C_{\eta_1} \le K_A \|L\| + K_B, \quad (16)$$

where $K_A > 0\ (= 0.001)$ and $K_B > 0\ (= 0.001)$ are constant and obtained indirectly from the CAD software, Pro-E,

$$C_{\eta_1} = \left[C_{\eta_{11}}(v,\eta) + D_{\eta_{11}}(v,\eta)\right], \quad (17)$$

$\|\cdot\|$ being the Euclidean norm and $L = [e\ \dot{e}]^T$.

4.3. Controller Design and Stability Analysis of the Actuated Dynamic. Implementing the control law into (11) yields

$$\ddot{e} = M_{\eta_1}^{-1} C_{\eta_1} \dot{e} - M_{\eta_1}^{-1}\Big[K_p e + K_i \int_0^\tau e\,\mathrm{d}t + K_d \frac{\mathrm{d}e}{\mathrm{d}t}\Big]. \quad (18)$$

State-space equations become

$$\begin{aligned} x_1 &= \int_0^\tau e^T\,\mathrm{d}t, \quad \dot{x}_1 = e^T,\\ x_2 &= e^T, \qquad\qquad \dot{x}_2 = \dot{e}^T,\\ x_3 &= \dot{e}^T,\\ \dot{x}_3 &= \ddot{e}^T\\ &= M_{\eta_1}^{-1} C_{\eta_1} x_3 - M_{\eta_1}^{-1} K_d x_3 - M_{\eta_1}^{-1} K_p x_2\\ &\quad - M_{\eta_1}^{-1} K_i x_1, \end{aligned} \quad (19)$$

where the superscript T in e^T indicates the transpose of e. Equation (19) in the matrix form becomes

$$\begin{bmatrix} \dot{x}_1\\ \dot{x}_2\\ \dot{x}_3 \end{bmatrix} = \overbrace{\begin{bmatrix} 0 & I_n & 0\\ 0 & 0 & I_n\\ -M_{\eta_1}^{-1}K_i & -M_{\eta_1}^{-1}K_p & -M_{\eta_1}^{-1}(K_d + C_{\eta_1}) \end{bmatrix}}^{\mathbf{A}} \begin{bmatrix} x_1\\ x_2\\ x_3 \end{bmatrix}. \quad (20)$$

To analyze the system's robust stability, consider the following Lyapunov function:

$$\begin{aligned} V(x) &= x^T P x\\ &= \frac{1}{2}\Big[\alpha_2 \int_0^t e(\tau)\,\mathrm{d}\tau + \alpha_1 e + \dot{e}\Big]^T M_{\eta_1}\\ &\quad \times \Big[\alpha_2 \int_0^t e(\tau)\,\mathrm{d}\tau + \alpha_1 e + \dot{e}\Big] + \varpi^T P_1 \varpi, \end{aligned} \quad (21)$$

where

$$\varpi = \begin{bmatrix} \int_0^t e(\tau)\,\mathrm{d}\tau\\ e \end{bmatrix}, \qquad P_1 = \frac{1}{2}\begin{bmatrix} \alpha_2 K_p + \alpha_1 K_i & \alpha_2 K_d + K_i\\ \alpha_2 K_d + K_i & \alpha_1 K_d + K_p \end{bmatrix}. \quad (22)$$

Hence

$$P = \frac{1}{2} \times \begin{bmatrix} \alpha_2 K_p + \alpha_1 K_i + \alpha_2^2 M_{\eta_1} & \alpha_2 K_d + K_i + \alpha_1\alpha_2 M_{\eta_1} & \alpha_2 M_{\eta_1}\\ \alpha_2 K_d + K_i + \alpha_1\alpha_2 M_{\eta_1} & \alpha_1 K_d + K_p + \alpha_1^2 M_{\eta_1} & \alpha_1 M_{\eta_1}\\ \alpha_2 M_{\eta_1} & \alpha_1 M_{\eta_1} & M_{\eta_1} \end{bmatrix}. \quad (23)$$

Since M_{η_1} is a positive definite matrix, P is positive definite if, and only if, P_1 is positive definite. Now choose $K_p = k_p I,\ K_d = k_d I$ and $K_i = k_i I$ such that P in (23), i.e.,

$$\begin{bmatrix} \alpha_2 k_p + \alpha_1 k_i & \alpha_2 k_d + k_i\\ \alpha_2 k_d + k_i & \alpha_1 k_d + k_p \end{bmatrix} \quad (24)$$

becomes positive definite. The following lemma gives the conditions for $V(x)$ to become positive definite, bounded from above and below.

Lemma 1. *Assume that the following inequalities hold:*

$$\begin{aligned} &\alpha_1 > 0, \quad \alpha_2 > 0, \quad \alpha_1 + \alpha_2 < 1,\\ s_1 &= \alpha_2(k_p - k_d) - (1-\alpha_1)k_i\\ &\quad - \alpha_2(1+\alpha_1-\alpha_2)\overline{m_{\eta_1}} > 0, \end{aligned} \quad (25)$$

$$\begin{aligned} s_2 &= k_p + (\alpha_1-\alpha_2)k_d - k_i\\ &\quad - \alpha_1(1+\alpha_2-\alpha_1)\overline{m_{\eta_1}} > 0. \end{aligned} \quad (26)$$

Then P is positive definite and satisfies the following inequality (Rayleigh-Ritz) :

$$\underline{\lambda}(P)\|x\|^2 \le V(x) \le \overline{\lambda}(P)\|x\|^2, \quad (27)$$

in which

$$\underline{\lambda}(P) = \min\Big\{\frac{1-\alpha_1-\alpha_2}{2} m_{\eta_1}, \frac{s_1}{2}, \frac{s_2}{2}\Big\}, \quad (28)$$

$$\overline{\lambda}(P) = \max\Big\{\frac{1+\alpha_1+\alpha_2}{2} m_{\eta_1}, \frac{s_3}{2}, \frac{s_4}{2}\Big\}, \quad (29)$$

and

$$\begin{aligned} s_3 &= \alpha_2(k_p + k_d) + (1+\alpha_1)k_i\\ &\quad + (1+\alpha_1+\alpha_2)\alpha_2\overline{m_{\eta_1}}, \end{aligned} \quad (30)$$

$$\begin{aligned} s_4 &= \alpha_1\overline{m_{\eta_1}}(1+\alpha_1+\alpha_2)\\ &\quad + (\alpha_1+\alpha_2)k_d + k_p + k_i. \end{aligned} \quad (31)$$

Since P is positive definite,

$$\begin{aligned}\dot{V}(x) = {} & x^T(A^TP + PA + \dot{P})x \\ & - x^TQx \\ & + \frac{1}{2}x^T \begin{bmatrix} \alpha_2 I \\ \alpha_1 I \\ I \end{bmatrix} \dot{M}_{\eta_1} \begin{bmatrix} \alpha_2 I & \alpha_1 I & I \end{bmatrix} x \\ & + \frac{1}{2}x^T \begin{bmatrix} 0 & \alpha_2^2 I & \alpha_1\alpha_2 I \\ \alpha_2^2 I & 2\alpha_1\alpha_2 I & (\alpha_1^2+\alpha_2)I \\ \alpha_1\alpha_2 I & (\alpha_1^2+\alpha_2)I & \alpha_1 I \end{bmatrix} \\ & \times \begin{bmatrix} M_{\eta_1} & 0 & 0 \\ 0 & M_{\eta_1} & 0 \\ 0 & 0 & M_{\eta_1} \end{bmatrix} x. \end{aligned} \tag{32}$$

Owing to $\dot{M}_{\eta_1} = 0$, (32) yields

$$\dot{V}(x) \le -\gamma\|x\|^2 + \zeta_2\overline{m}_{\eta_1}\|x\|^2 \tag{33}$$

and

$$\gamma = \min\left\{\alpha_2 k_i, \alpha_1 k_p - \alpha_2 k_d - k_i, k_d\right\}. \tag{34}$$

Let $\|L\| \le \|x\|$. Denote by $\lambda_2 = \overline{\lambda}(R_2)$ the largest eigenvalue of R_2,

$$R_2 = \begin{bmatrix} 0 & \alpha_2^2 I & \alpha_1\alpha_2 I \\ \alpha_2^2 I & 2\alpha_1\alpha_2 I & (\alpha_1^2+\alpha_2)I \\ \alpha_1\alpha_2 I & (\alpha_1^2+\alpha_2)I & \alpha_1 I \end{bmatrix}. \tag{35}$$

As a result, the error system of the RRC ROV II, (20), is rendered GAS, if λ_2 is chosen small enough and the control gains K_p, K_d and K_i are large enough. The next step is to show that unactuated dynamics are exponentially bounded.

5. Exponential Stability of Unactuated Dynamics Using Sørdalen's Lemma

As was shown in Section 4, the term $h_2(\dot{e}, e, t)$ consists of $\dot{e}$ and e converged exponentially to zero, i.e., $\dot{e}, e \to 0$ as $t \to 0$, yielding $\ddot{\eta}_u = f_2(\dot{\eta}_u, \eta_u, t) + B_{\eta_u}u_u$. The solution of the tracking error, e, can be approximated as $e = C^e e^{-\gamma_e t} \Rightarrow \dot{e} = C^{\dot{e}} e^{-\gamma_{\dot{e}} t}$ and, by substituting it into $h_2(\dot{e}, e, t)$, yields

$$\begin{aligned} h_2(\dot{e}, e, t) = {} & -\frac{M_{\eta_{12}} C_{\eta_{12}}}{M_{\eta_{22}} M_{\eta_{11}} - M_{\eta_{12}}^2} C^e e^{-\gamma_e t} + M_{\eta_{11}} g_{\eta_u} \\ & + M_{\eta_{11}} B_{\eta_2} u_u \to 0 \end{aligned} \tag{36}$$

for $u_u = -B_{\eta_2}^{-1} g_{\eta_u}$. The initial assumption $h_1(\dot{\eta}_u, \eta_u, t) \to 0$ as $t \to \infty$ can be validated by checking the asymptotic stability of η_u. First, decompose η_u into two part as follows:

$$\ddot{\eta}_u = \begin{bmatrix} \ddot{\phi} \\ \ddot{\theta} \end{bmatrix} = \begin{bmatrix} f_{\dot{\phi}}(\dot{\phi}, \phi, t) + d_{\dot{\phi}}(t) \\ f_{\dot{\theta}}(\dot{\theta}, \theta, t) + d_{\dot{\theta}}(t) \end{bmatrix}, \tag{37}$$

where $d_{\dot{\phi}}(t), d_{\dot{\theta}}(t)$ are considered as perturbations on $\dot{\phi}$ and $\dot{\theta}$, respectively. The proof of the exponential bound of the unactuated subsystems can be obtained as shown below. The definite integral of $f_{\dot{\phi}}(\dot{\phi}, \phi, t)$ from the time 0 to t becomes

$$\begin{aligned} \left|\int_0^t f_{\dot{\phi}}(\dot{\phi}, \phi, \tau)\,\mathrm{d}\tau\right| \le {} & \int_0^t \left|f_{\dot{\phi}_{I1}} \frac{\partial\psi}{\partial\tau}/k_{a1}\right| + \left|f_{\dot{\phi}_{I2}} \frac{\partial\phi}{\partial\tau}/k_{a1}\right| \\ & + \left|f_{\dot{\phi}_{I3}} \frac{\partial\theta}{\partial\tau}/k_{a1}\right| + |f_{\dot{\phi}_{I4}}|\,\mathrm{d}\tau, \end{aligned} \tag{38}$$

where $k_{a1} f_{\dot{\phi}_{I1}}$, $f_{\dot{\phi}_{I2}}$, $f_{\dot{\phi}_{I3}}$, $f_{\dot{\phi}_{I4}}$ can be found in Appendix. Substituting I_{xx}, I_{xy}, I_{xz}, I_{yz}, $\dot{\psi}$, $\dot{\phi}$ and $\dot{\theta}$ into the preceding equation gives

$$\begin{aligned} \left|\int_0^t f_{\dot{\phi}}(\dot{\phi}, \phi, \tau)\,\mathrm{d}\tau\right| \le {} & \int_0^t |\beta_1\dot{\theta}| + |\beta_2\dot{\psi}| + |\beta_3\dot{\phi}|\,\mathrm{d}\tau \\ \le {} & \int_0^t \beta_1 |C^{\dot{\theta}} e^{-\alpha_{\dot{\theta}}\tau}| + \beta_2 |C^{\dot{\psi}} e^{-\alpha_{\dot{\psi}}\tau}| \\ & + \beta_3 |C^{\dot{\phi}} e^{-\alpha_{\dot{\phi}}\tau}| + \beta_4\,\mathrm{d}\tau, \\ \left|\int_0^t f_{\dot{\phi}}(\dot{\phi}, \phi, \tau) + \epsilon_{\dot{\phi}}\,\mathrm{d}\tau\right| \le {} & \beta_1 \frac{C^{\dot{\theta}}}{\alpha_{\dot{\theta}}} + \beta_2 \frac{C^{\dot{\psi}}}{\alpha_{\dot{\psi}}} + \beta_3 \frac{C^{\dot{\phi}}}{\alpha_{\dot{\phi}}}, \end{aligned} \tag{39}$$

where $\beta_1,\ \beta_2,\ \beta_3,\ \beta_4 > 0$. In the RRC ROV II, $\beta_1 = 15603,\ \beta_2 = 15470,\ \beta_3 = 2.7,\ \beta_4 = 1650$. Then $d_{\dot{\phi}}(t)$ in (37) becomes

$$\begin{aligned} |d_{\dot{\phi}}(t)| = {} & |f_{\dot{z}_1}\dot{z} + f_{\dot{x}_1}\dot{x} + f_{\dot{y}_1}\dot{y} + f_{\dot{\psi}_1}\dot{\psi} + f_{\dot{\theta}_1}\dot{\theta}| \\ \le {} & |f_{\dot{z}_1}\dot{z}| + |f_{\dot{x}_1}\dot{x}| + |f_{\dot{y}_1}\dot{y}| \\ & + |f_{\dot{\psi}_1}\dot{\psi}| + |f_{\dot{\theta}_1}\dot{\theta}|. \end{aligned} \tag{40}$$

Define

$$\begin{aligned} \gamma_{\dot{\phi}} = \min\big\{ & \alpha^{\dot{z}} + \alpha^{\dot{x}}, \alpha^{\dot{z}} + \alpha^{\dot{y}}, \alpha^{\dot{x}} + \alpha^{\dot{y}}, \alpha^{\dot{\psi}} + \alpha^{\dot{\theta}}, \alpha^{\dot{\psi}} \\ & + \alpha^{\dot{\phi}}, \alpha^{\dot{\theta}} + \alpha^{\dot{\phi}}, \alpha^{\dot{z}}, \alpha^{\dot{x}}, \alpha^{\dot{y}}, \alpha^{\dot{\psi}}, \alpha^{\dot{\phi}}, \alpha^{\dot{\theta}}\big\} \end{aligned} \tag{41}$$

and $\dot{z} = C^{\dot{z}} e^{-\gamma_{\dot{z}}}$, $\dot{x} = C^{\dot{x}} e^{-\gamma_{\dot{x}}}$, $\dot{y} = C^{\dot{y}} e^{-\gamma_{\dot{y}}}$, $\dot{\psi} = C^{\dot{\psi}} e^{-\gamma_{\dot{\psi}}}, \forall\alpha^{\dot{z}}, \alpha^{\dot{x}}, \alpha^{\dot{y}}, \alpha^{\dot{\psi}}$, where $C^{\dot{z}}, C^{\dot{x}}, C^{\dot{y}}, C^{\dot{\psi}} > 0$ (Kreyszig, 1998) for an exponentially stable system. Then

$$|d_{\dot{\phi}}(t)| \le D e^{-\gamma_{\dot{\phi}} t}. \tag{42}$$

The solution of $\ddot{\phi}(t)$ becomes

$$|\dot{\phi}(t)| = \Big| e^{-[f_{\dot{\phi}}(\dot{\phi},\phi,t)+\epsilon_{\dot{\phi}}]t}\dot{\phi}(0) + \int_0^t e^{-[f_{\dot{\phi}}(\dot{\phi},\phi,t)+\epsilon_{\dot{\phi}}]\tau} d_{\dot{\phi}}(\tau)\,\mathrm{d}\tau \Big| \le e^{-P_{\dot{\phi}}t}|\dot{\phi}(0)| + \left| \int_0^t e^{-P_{\dot{\phi}}\tau} d_{\dot{\phi}}(\tau)\,\mathrm{d}\tau \right| \le e^{-P_{\dot{\phi}}t}|\dot{\phi}(0)| + \frac{|D[e^{-(P_{\dot{\phi}}+\gamma_{\dot{\phi}})t}-1]|}{|P_{\dot{\phi}}+\gamma_{\dot{\phi}}|}, \quad (43)$$

where $P_{\dot{\phi}} = \int_0^t [f_{\dot{\phi}}(\dot{\phi},\phi,\tau) + \epsilon_{\dot{\phi}}]\,\mathrm{d}\tau$. Thus $\dot{\phi}(t)$ is bounded for any $t \ge 0$. Also, $\dot{\phi}(t) \to 0$ since $1/|P_{\dot{\phi}} + \gamma_{\dot{\phi}}|$ is small.

Next, to show that $\phi(t)$ is bounded, consider

$$|\phi(t)| = \left| \int_0^t \dot{\phi}(t)\,\mathrm{d}\tau + \phi(0) \right| \le \int_0^t |\dot{\phi}(t)|\,\mathrm{d}\tau + |\phi(0)|. \quad (44)$$

Using (43), we get

$$|\phi(t)| \le \int_0^t e^{-P_{\dot{\phi}}\tau}\,\mathrm{d}\tau|\dot{\phi}(0)| + \frac{D}{|P_{\dot{\phi}}+\gamma_{\dot{\phi}}|}\int_0^t (e^{-(P_{\dot{\phi}}+\gamma_{\dot{\phi}})\tau}-1)\,\mathrm{d}\tau + |\phi(0)| \le -\frac{e^{-P_{\dot{\phi}}\tau}+1}{P_{\dot{\phi}}}|\dot{\phi}(0)| - \frac{D}{|P_{\dot{\phi}}+\gamma_{\dot{\phi}}|^2}e^{-(P_{\dot{\phi}}+\gamma_{\dot{\phi}})t} - \frac{D}{|P_{\dot{\phi}}+\gamma_{\dot{\phi}}|}(t-1) + |\phi(0)|. \quad (45)$$

Thus, $\phi(t)$ is bounded for all $t \ge 0$ as $1/|P_{\dot{\phi}} + \gamma_{\dot{\phi}}|$ is small for the RRC ROV II.

Repeat the same procedure from (38) to (45) for $f_{\dot{\theta}}(\dot{\theta},\theta,\tau)$. Substituting $I_{xx}, I_{xy}, I_{xz}, I_{yz}$, see (Koh *et al.*, 2002a), $\dot{\psi}, \dot{\phi}$ and $\dot{\theta}$ into the preceding equation gives the definite integral of $f_{\dot{\phi}}(x,t)$,

$$\left| \int_0^t f_{\dot{\theta}}(\dot{\theta},\theta,\tau)\,\mathrm{d}\tau \right| = \left| \int_0^t f_{\dot{\theta}_1}\,\mathrm{d}\tau \right| \le \int_0^t |\alpha_1\dot{\theta}| + |\alpha_2\dot{\psi}| + |\alpha_3\dot{\phi}| + |\alpha_4|\,\mathrm{d}\tau \le \int_0^t \alpha_1 C^{\dot{\theta}} e^{-\alpha_{\dot{\theta}}\tau} + \alpha_2 C^{\dot{\psi}} e^{-\alpha_{\dot{\psi}}\tau} + \alpha_3 C^{\dot{\phi}} e^{-\alpha_{\dot{\phi}}\tau} + \alpha_4\,\mathrm{d}\tau, \quad (46)$$

$$\left| \int_0^t [f_{\dot{\theta}}(\dot{\theta},\theta,\tau) + \epsilon_{\dot{\theta}}]\,\mathrm{d}\tau \right| \le \alpha_1\frac{C^{\dot{\theta}}}{\alpha_{\dot{\theta}}} + \alpha_2\frac{C^{\dot{\psi}}}{\alpha_{\dot{\psi}}} + \alpha_4\frac{C^{\dot{\phi}}}{\alpha_{\dot{\phi}}}, \quad (47)$$

where $\alpha_1, \alpha_2, \alpha_3, \alpha_4 > 0$. In RRC ROV II, $\alpha_1 = 25.8$, $\alpha_2 = 12270.8$, $\alpha_3 = 12529$, $\alpha_4 = 260378$. Then $d_{\dot{\theta}}(t)$ in (37) becomes

$$|d_{\dot{\theta}}(t)| = |f_{\dot{z}_2}\dot{z} + f_{\dot{x}_2}\dot{x} + f_{\dot{y}_2}\dot{y} + f_{\dot{\psi}_2}\dot{\psi} + f_{\dot{\phi}_2}\dot{\phi}| \le |f_{\dot{z}_2}\dot{z}| + |f_{\dot{x}_2}\dot{x}| + |f_{\dot{y}_2}\dot{y}| + |f_{\dot{\psi}_2}\dot{\psi}| + |f_{\dot{\phi}_2}\dot{\phi}|. \quad (48)$$

Define

$$\gamma_{\dot{\theta}} = \min\{\alpha^{\dot{z}} + \alpha^{\dot{x}}, \alpha^{\dot{z}} + \alpha^{\dot{y}}, \alpha^{\dot{x}} + \alpha^{\dot{y}}, \alpha^{\dot{\psi}} + \alpha^{\dot{\theta}}, \alpha^{\dot{\psi}} + \alpha^{\dot{\phi}}, \alpha^{\dot{\theta}} + \alpha^{\dot{\phi}}, \alpha^{\dot{z}}, \alpha^{\dot{x}}, \alpha^{\dot{y}}, \alpha^{\dot{\psi}}, \alpha^{\dot{\phi}}, \alpha^{\dot{\theta}}\}, \quad (49)$$

and $\dot{z} = C^{\dot{z}}e^{-\gamma_{\dot{z}}}$, $\dot{x} = C^{\dot{x}}e^{-\gamma_{\dot{x}}}$, $\dot{y} = C^{\dot{y}}e^{-\gamma_{\dot{y}}}$, $\dot{\psi} = C^{\dot{\psi}}e^{-\gamma_{\dot{\psi}}}$, $\forall \alpha^{\dot{z}}, \alpha^{\dot{x}}, \alpha^{\dot{y}}, \alpha^{\dot{\psi}}$, where $C^{\dot{z}}, C^{\dot{x}}, C^{\dot{y}}, C^{\dot{\psi}} > 0$ (Kreyszig, 1998) for an exponentially stable system. Then

$$|d_{\dot{\theta}}(t)| \le De^{-\gamma_{\dot{\theta}}t}. \quad (50)$$

The solution of $\ddot{\theta}(t)$ becomes

$$|\dot{\theta}(t)| = \Big| e^{-[f_{\dot{\theta}}(\dot{\theta},\theta,t)+\epsilon_{\dot{\theta}}]t}\dot{\theta}(0) + \int_0^t e^{-[f_{\dot{\theta}}(\dot{\theta},\theta,t)+\epsilon_{\dot{\theta}}]\tau} d_{\dot{\theta}}(\tau)\,\mathrm{d}\tau \Big| \le e^{-P_{\dot{\theta}}t}|\dot{\theta}(0)| + \left| \int_0^t e^{-P_{\dot{\theta}}\tau} d_{\dot{\theta}}(\tau)\,\mathrm{d}\tau \right| \le e^{-P_{\dot{\theta}}t}|\dot{\theta}(0)| + \frac{|D[e^{(P_{\dot{\phi}}+\gamma_{\dot{\phi}})t}-1]|}{|P_{\dot{\phi}}+\gamma_{\dot{\phi}}|}, \quad (51)$$

where $P_{\dot{\theta}} = \int_0^t [f_{\dot{\theta}}(\dot{\theta},\theta,\tau) + \epsilon_{\dot{\theta}}]\,\mathrm{d}\tau$. Thus $\dot{\theta}(t)$ is bounded for any $t \ge 0$. Also, $\dot{\theta}(t) \to 0$ as $1/|P_{\dot{\theta}} + \gamma_{\dot{\theta}}|$ is small. Next, to show that $\theta(t)$ is bounded, consider

$$|\theta(t)| = \left| \int_0^t \dot{\theta}(t)\,\mathrm{d}\tau + \theta(0) \right| \le \int_0^t |\dot{\theta}(t)|\,\mathrm{d}\tau + |\theta(0)|. \quad (52)$$

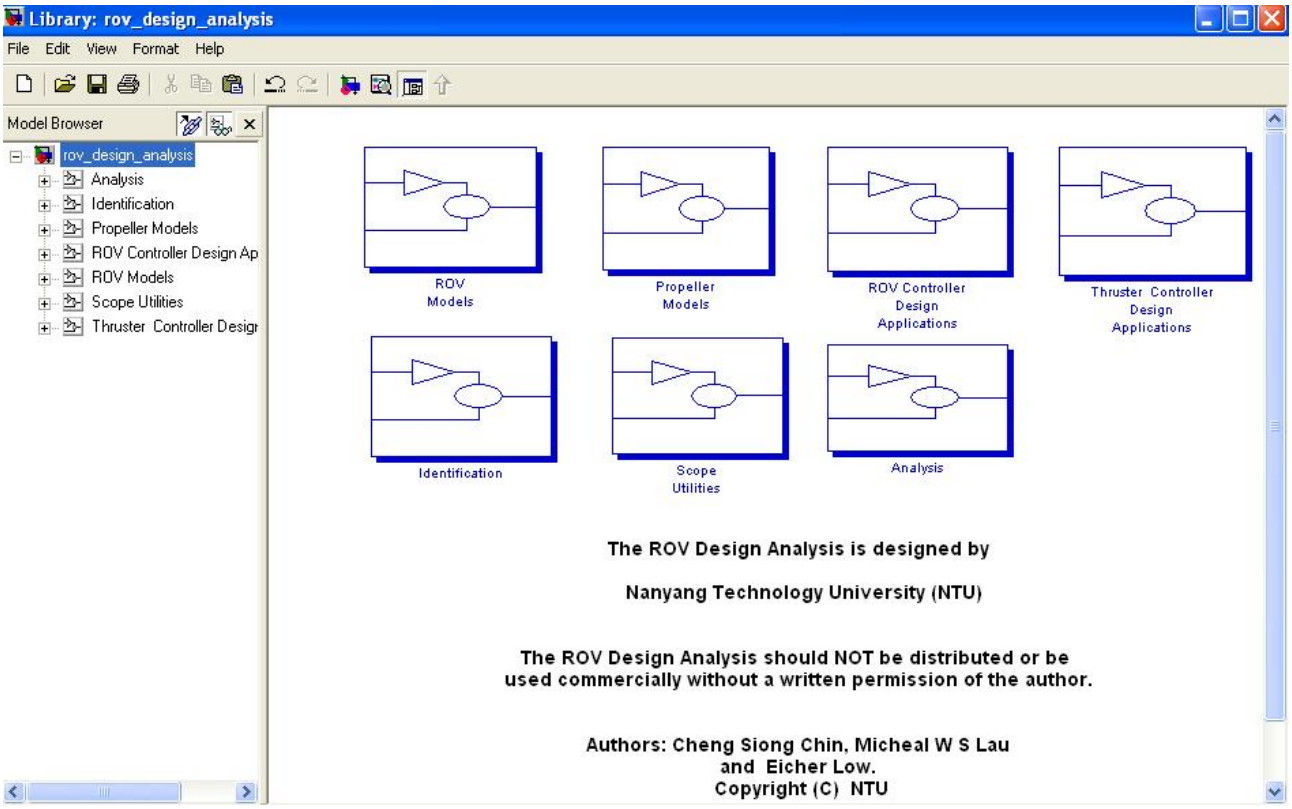

Fig. 3. SIMULINK library browser showing the RDA package.

Using (51), we have

$$\begin{aligned}|\theta(t)| &\le \frac{1}{|P_{\dot\theta}+\gamma_{\dot\theta}|}\int_0^t e^{-(P_{\dot\theta}+\gamma_{\dot\theta})\tau}\,\mathrm{d}\tau \\ &\quad + \int_0^t e^{-P_{\dot\theta}\tau}\,\mathrm{d}\tau|\dot\theta(0)| \\ &\quad + \int_0^t \frac{1}{|P_{\dot\theta}+\gamma_{\dot\theta}|}\,\mathrm{d}\tau + |\theta(0)| + |\theta(0)| \\ &\le -\frac{e^{-P_{\dot\theta}\tau}+1}{P_{\dot\theta}}|\dot\theta(0)| - \frac{D}{|P_{\dot\theta}+\gamma_{\dot\theta}|^2}e^{-(P_{\dot\theta}+\gamma_{\dot\theta})t} \\ &\quad - \frac{D}{|P_{\dot\theta}+\gamma_{\dot\theta}|}(t-1) + |\theta(0)|. \end{aligned} \tag{53}$$

Thus, $\theta(t)$ is bounded for any $t \ge 0$ as $1/|P_{\dot\theta}+\gamma_{\dot\theta}|$ is small for the RRC ROV II.

6. Computer Simulation Results

This section illustrates the performance of the proposed control scheme (in the presence of parameter perturbations) using the ROV Design and Analysis (RDA) package (see Fig. 3) developed at the NTU. The platform adopted for the development of RDA is MATLAB/SIMULINK. RDA provides the necessary resources for a rapid and systematic implementation of mathematical models of ROV systems with the focus on ROV modeling, control system design and analysis. The package provides examples ready for simulation. As is shown in Fig. 4, the block diagram of the proposed robust PID control was designed.

The performance of the proposed control scheme was investigated in computer simulations using a Pentium IV, 2.4 GHz computer. The simulation time was set to 100 s. The RRC ROV II parameters used in simulations can be found in (Koh *et al.*, 2002b). As the vehicle is currently equipped only with limited sensors, the desired position command values, $v = [0.5\ 0\ 1\ 0\ 0\ 0]^T$, are chosen with this purpose in mind. The objective is to regulate the position of the RRC ROV II to $x = 0.5\,\mathrm{m}$ and $z = 1\,\mathrm{m}$ or the error signal equal to zero.

The PID was selected due to its simplicity in implementation and its wide use in control applications. The control algorithm requires reduced computing resources, and is therefore suited for an on-board implementation. The PID control parameters were obtained from the Response Optimization (using the gradient descent method) toolbox in SIMULINK. The PID parameters are as follows: $K_p = \mathrm{diag}\{11, 11, 9, 1\}$, $K_i = \mathrm{diag}\{2, 4, 1, 2\}$ and $K_d = \mathrm{diag}\{1, 1, 2, 1\}$. For example, the optimization

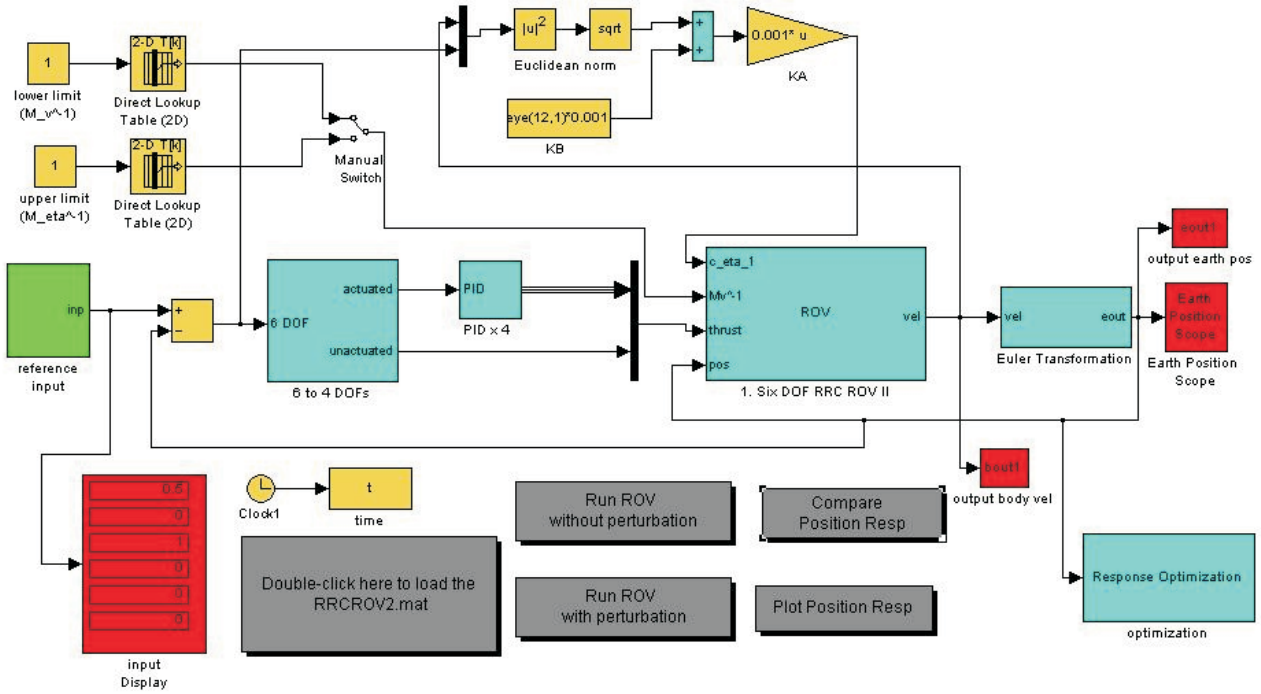

Fig. 4. SIMULINK block diagram of the proposed robust PID control.

setting for the response in the x-direction was constrained as shown in Fig 7.

As was already mentioned, the system is separated into actuated and unactuated states. In SIMULINK, it is modeled as a selector that channels the actuated and unactuated states into two paths. The PID is used only for the actuated states while the unactuated ones are left uncontrolled, since then are self-stabilizable. The "robust" PID controller is called this way due to the perturbation of the mass inertia term as in (14). The perturbation of the mass inertia term ranges from the minimum to the maximum of the scale ($-0.001 \leq M_{\eta_1}^{-1} \leq 0.01$). This can be modeled as a two-dimensional (2D) look-up table as shown in Fig. 4. During simulations, only the maximum value (or a worst-case perturbation) is used. Similarly, the perturbation for the centripetal, Coriolis and hydrodynamic damping matrix was set at ($C_{\eta_1} \leq 0.001\|L\| + 0.001$).

Figure 5 shows simulation results for the robust PID control design with and without perturbations. It shows the position of the ROV with respect to the inertia frame. As can be observed, the ROV control system is able to regulate about the selected reference position. The roll and pitch motions are self-stabilizable about the zero position (as seen in Sørdalen's proof). From Fig. 5 it can be seen that actuated states exhibit asymptotically stable phenomena, as proved by the Lyapunov stability theory. Notice that, in spite of parameter uncertainty, the ROV converges asymptotically to the desired position.

The flow chart shown in Fig. 6 illustrates the robust PID design flow and methodology using RDA for the RRC ROV II. PID parameters are tuned off-line by the Response Optimization toolbox using gradient descent till the desired responses are obtained. Besides, the tuning of PID parameters can be performed iteratively.

7. Conclusion

Besides using the ROV's body-fixed coordinates in stability analysis, the earth-fixed coordinate model was analyzed. The stabilizability condition of the underactuated ROV was shown. The nonlinear system was separated into actuated and unactuated dynamic equations, and the asymptotical stability of closed-loop actuated equations, using the robust PID controller in the earth-fixed frame, was examined. This is based on the argument that the actuated dynamic equation could converge exponentially to zero by the PID controller. The asymptotic stability proof by Sørdalen in the unactuated dynamic equation provides a validation for the initial argument of the roll and pitch dynamics convergence to zero. The vehicle in the earth-fixed frame with self-stabilizable unactuated dynamics is globally asymptotically stable with the robust PID controller in actuated dynamics. This gives a necessary and sufficient condition for the GAS of the ROV in the earth-fixed frame.

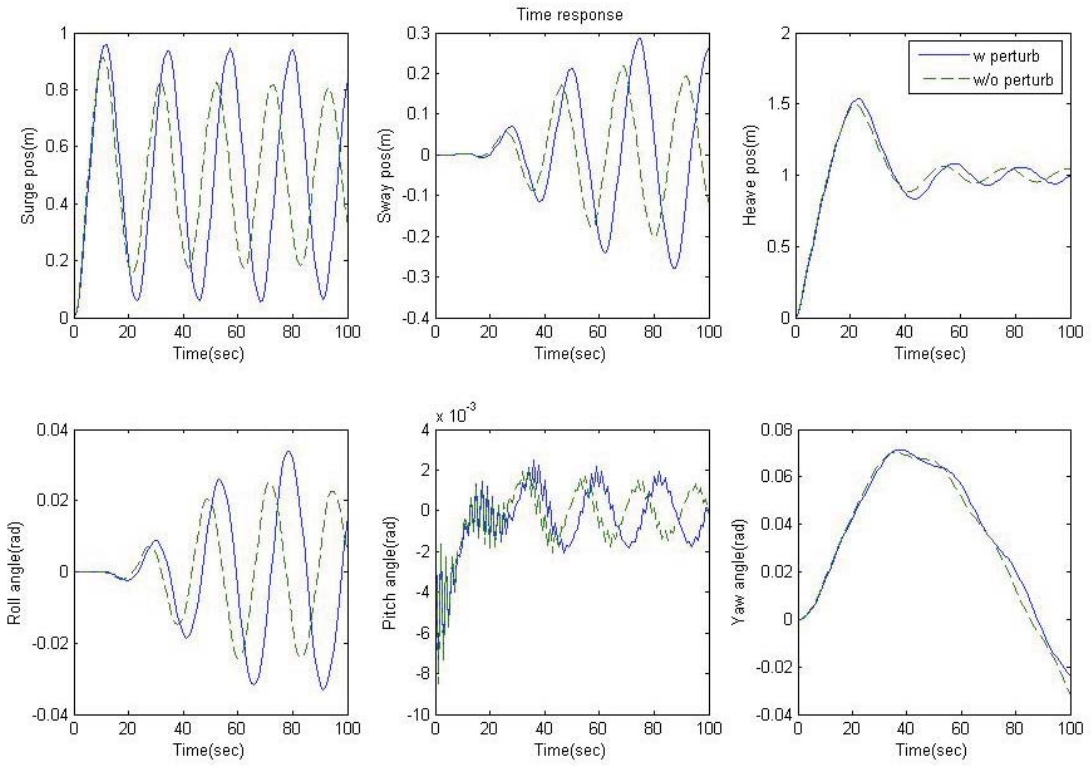

Fig. 5. Position response of the proposed robust PID control for $x = 0.5$ m and $z = 1$ m.

By simulating closed-loop control system design using the RDA package, the asymptotical stability of the robust PID controller for the RRC ROV II can be observed as position responses converge asymptotically to the desired position. The PID is said to be robust as the ROV's mass inertia, centripetal and Coriolis matrix and the diagonal hydrodynamic damping matrix were allowed to vary within the limits obtained explicitly from the CAD software, Pro-E.

In summary, the RDA provides a systematic methodology in control system simulation and stability analysis before implementation. It also provides necessary resources for a rapid implementation of mathematical models of ROV systems. The proposed control algorithm is quite simple and requires little computing resources, and is therefore suited for an on-board implementation. Simulation results show the effectiveness of the proposed methodology. If the real-time tuning of PID parameters is used, the control system could be more robust against larger parameters perturbation. As is shown in this paper, PID parameters can be conveniently tuned by the Response Optimization toolbox in MATLAB/SIMULINK instead of the trial-and-error method of tuning.

Acknowledgments

The authors would like to thank and acknowledge the contributions by all project team members from the NTU Robotics Research Centre, especially Mr. Lim Eng Cheng, Ms. Agnes S.K. Tan, Ms. Ng Kwai Yee and Mr. You Kim San.

References

Brockett R.W. (1983): *Asymptotic stability and feedback stabilization*, In: Differential Geometric Control Theory (R.W. Brockett, R.S. Millman and H.J. Sussmann, Eds.). — Boston: Birkhäuser, pp. 181–191.

Byrnes C. and Isidori A. (1991): *On the attitude stabilization of rigid spacecraft*. — Automatica, Vol. 27, No. 1, pp. 87–95.

Fossen T.I. (1994): *Guidance and Control of Ocean Vehicles*. — New York: Wiley.

Koh T.H., Lau M.W.S., Low E., Seet G.G.L. and Cheng P.L. (2002a): *Preliminary studies of the modeling and control of a twin-barrel underactuated underwater robotic vehicle*. — Proc. 7-th Int. Conf. *Control, Automation, Robotics Vision*, Singapore, pp. 1043–1047.

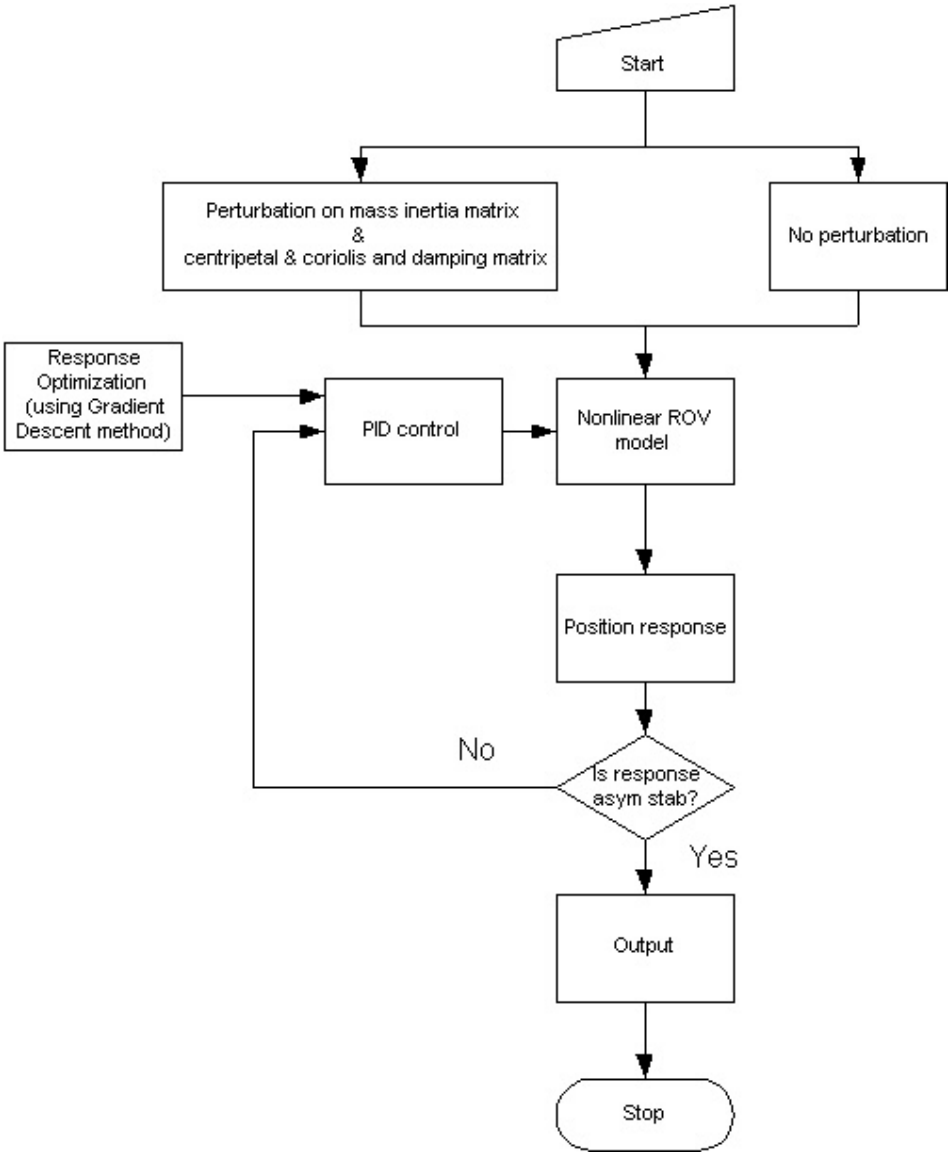

Fig. 6. Flow chart of the robust PID design flow and methodology using RDA on the RRC ROV II.

Koh T.H., Lau M.W.S., Low E., Seet G., Swei S. and Cheng P.L. (2002b): *Development and improvement of an underactuated remotely operated vehicle (ROV)* . — Proc. MTS/IEEE Int. Conf. *Oceans*, Biloxi, MS, pp. 2039–2044.

Kreyszig E. (1998): *Advanced Engineering Mathematics*. — New York: Wiley.

Lau M.W.S., Swei S.S.M., Seet S.S.M., Low E. and Cheng P.L. (2003): *Control of an underactuated remotely operated underwater vehicle*. — Proc. Inst. Mech. Eng., Part 1: J. Syst. Contr., Vol. 217, No. 1, pp. 343–358.

Søodalen O.J. and Egeland O. (1993): *Exponential stabilization of chained nonholonomic systems*. — Proc. 2-nd *European Control Conf.,* Groningen, The Netherlands, pp. 1438–1443.

Sødalen O.J. and Egeland O. (1995): *Exponential stabilization of nonholonomic chained systems*. — IEEE Trans. Automat. Contr., Vol. 40, No. 1, pp. 35–49.

Sørdalen O.J., Dalsmo M. and Egeland O. (1993): *An exponentially convergent control law for a nonholonomic underwater vehicle*. — Proc. 3-rd Conf. *Robotics and Automation, ICRA*, Atlanta, Georgia, USA, pp. 790–795.

Wichlund K.Y., Sørdalen O.J. and Egeland O. (1995): *Control of vehicles with second-order nonholonomic constraints: Underactuated vehicles*. — Proc. *European Control Conf.,* Rome, Italy, pp. 3086–3091.

Yuh J. (1990): *Modeling and control of underwater robotic vehicles*. — IEEE Trans. Syst. Man Cybern., Vol. 20, No. 6, pp. 1475–1483.

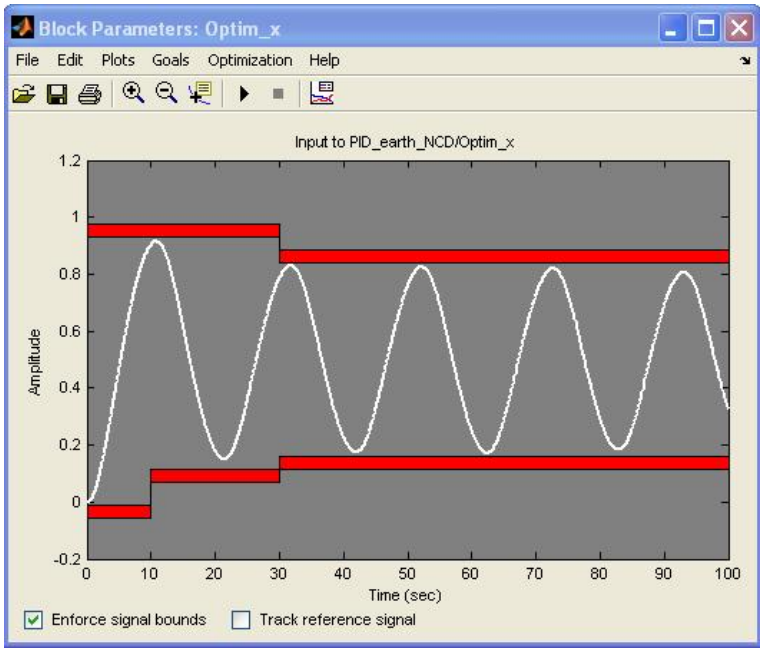

Fig. 7. Example of response optimization setting on the output x.

Appendix

The parameters used in (38) are as follows:

$$k_{a1} = -I_{xx}\,{I_{yz}}^2 + I_{xx}\,I_{yy}\,I_{zz} - 2\,I_{yz}\,I_{xy}\,I_{xz} - I_{yy}\,{I_{xz}}^2 - {I_{xy}}^2\,I_{zz},$$

$$\begin{aligned} f_{\dot{\phi}_{I1}} = {} & I_{xy}I_{yz}^2 - I_{xz}^2I_{zz} + I_{xy}I_{zz}^2 + I_{xy}^2I_{yy} - I_{yy}^2I_{xz} \\ & - I_{xx}I_{yy}^2 + I_{xy}^3 - I_{xz}^3 - 2I_{xy}I_{xz}I_{yy} \\ & - I_{xy}I_{yz}I_{yy} + I_{xx}I_{yz}I_{xz} + I_{xx}I_{zz}I_{xz} \\ & - I_{xx}I_{yy}I_{xy} + I_{yy}I_{xz}I_{yz} - I_{yz}^2I_{xz} + 2I_{xy}I_{zz}I_{xz} \\ & - I_{xy}I_{zz}I_{yz} + I_{xy}I_{xz}^2 + I_{xx}I_{zz}^2 - 2I_{xy}^2I_{yz} \\ & - I_{xy}^2I_{xz} + 2I_{yz}I_{xz}^2 - I_{xx}I_{yz}I_{xy} + I_{yz}I_{xz}I_{zz}, \end{aligned}$$

$$\begin{aligned} f_{\dot{\phi}_{I2}} = {} & -I_{xx}I_{zz}I_{xz} - I_{xy}I_{zz}I_{xz} - I_{xy}^3 - I_{xx}I_{yz}I_{xz} \\ & + I_{xy}^2I_{xz} + I_{xx}I_{yy}I_{xy} + I_{xx}I_{yz}I_{xy} + I_{xy}^2I_{yz} \\ & - I_{xy}I_{xz}^2 - I_{yz}I_{xz}^2 + I_{xy}I_{xz}I_{yy} + I_{xz}^3, \end{aligned}$$

$$\begin{aligned} f_{\dot{\phi}_{I3}} = {} & -3I_{xx}I_{yz}^2 - I_{xy}^2I_{zz} - I_{yy}I_{xz}^2 - 4I_{yz}I_{xy}I_{xz} \\ & + I_{xx}I_{yy}I_{zz} - I_{yy}I_{xz}I_{yz} - I_{xy}I_{zz}I_{yz} \\ & - I_{xy}I_{xz}I_{yy} - I_{xy}I_{yz}I_{yy} - 2I_{xx}I_{zz}I_{yz} \\ & - 2I_{xx}I_{yz}I_{yy} - I_{yz}^2I_{xz} - I_{xx}I_{yy}^2 - I_{yy}^2I_{xz} \\ & + I_{xy}^2I_{yz} - I_{xx}I_{zz}^2 - I_{xy}I_{zz}^2 + I_{yz}I_{xz}^2 \\ & + I_{xz}^2I_{zz} - I_{xy}I_{yz}^2 + I_{xy}^2I_{yy} - I_{yz}I_{xz}I_{zz} \\ & - I_{xy}I_{zz}I_{xz}, \end{aligned}$$

$$\begin{aligned} f_{\dot{\phi}_{I4}} = {} & (-I_{yz}I_{xz}Kp - I_{xy}I_{zz}Kp - I_{yy}I_{xz}Kp \\ & - KpI_{yy}I_{zz} - I_{yz}I_{xy}Kp + KpI_{yz}^2)/k_{a1}. \end{aligned}$$

Received: 19 Januar 2006
Revised: 11 April 2006
Re-revised: 8 June 2006